Available online at www.sciencedirect.com
SCIENCE DIRECT®
Bioorganic & Medicinal Chemistry 13 (2005) 1231–1238
Bioorganic & Medicinal Chemistry

# NMR conformational analysis of *p*-tolyl furanopyrimidine 2′-deoxyribonucleoside and crystal structure of its 3′,5′-di-*O*-acetyl derivative

Noor Esho,[a] Jean-Paul Desaulniers,[b] Brian Davies,[a] Helen M.-P. Chui,[b] Meneni Srinivasa Rao,[a] Christine S. Chow,[b] Slawomir Szafert[c,*] and Roman Dembinski[a,*]

[a]*Department of Chemistry and Center for Biomedical Research, Oakland University, 2200 N. Squirrel Rd, Rochester, MI 48309-4477, USA*
[b]*Department of Chemistry, Wayne State University, Detroit, MI 48202, USA*
[c]*Department of Chemistry, University of Wroclaw, F. Joliot-Curie 14, 50-383 Wroclaw, Poland*

Received 16 September 2004; revised 8 November 2004; accepted 8 November 2004

**Abstract**—The conformation of a representative molecule of a new, potent class of antiviral-active modified nucleosides is determined. A bicyclic nucleoside, 3-(2′-deoxy-β-D-ribofuranosyl)-6-(4-methylphenyl)-2,3-dihydrofuro[2,3-*d*]pyrimidin-2-one, shows C2′-*endo* and C3′-*endo* ribose conformations in solution (63:37, 37 °C; DMSO-$d_6$), as determined by $^1$H NMR studies. The crystal structure of a 3′,5′-di-*O*-acetyl-protected derivative (monoclinic, $P2_1$, $a/b/c$ = 6.666(1)/12.225(1)/24.676(2) Å, $\beta$ = 90.24(1)°, $Z$ = 4) shows exclusively C2′-*endo* deoxyribose puckering. The base is found in the *anti* position both in solution and in crystalline form.


## 1. Introduction

X-ray crystallographic and NMR methods are frequently used to support the drug-discovery process. Thus, the determination of conformation for compounds with biological activity provides useful information for the development of new structures with interesting properties.[1] The conformational preferences of nucleosides may be important for their biological roles. In viral diseases, the enzymes appear to have strict conformational requirements. For example, there is an increasing amount of experimental evidence that the herpes thymidine kinase (HSV-TK) and cellular DNA polymerases discriminate their substrates on the basis of the nucleoside conformation, in particular the geometry adopted by the furanose ring.[2]

Elucidation of the biological properties of 5-alkynyl uridine analogs resulted in numerous activity reports[3] and detailed synthetic studies.[4,5] It was noted that, when starting from 5-iodouridine (**1**), synthesis of 5-alkynyl uridine derivatives (**2**) via Sonogashira coupling also leads to the formation of a side product identified as furanopyrimidine (**3**, Scheme 1).[4c,d,6,7] An increasing interest in **3** has resulted from its identification as an extremely potent and selective antiviral agent. In particular, the C6-substituted bicyclic structure **3** exhibits significant therapeutic potential,[8,9] which is attributed to the chemical bypass mechanism of the nucleoside kinase.[9b,e,10] A variety of nucleoside **3** derivatives with different substituents at C6 have been synthesized, and their antiviral properties have been examined in systematic structure–activity studies.[8,9a,d] In particular, the ability of *p*-(*n*-alkyl)phenyl furanopyrimidines to inhibit the replication of strains of thymidine kinase-competent (TK+) or -deficient (TK-) varicella-zoster virus (VZV) surpassed ca. $10^4$ times acyclovir or bromovinyldeoxyuridine.[8a] Low cytotoxicity leads to selectivity index values exceeding $10^6$ for the most active compounds.[8a] It is likely that the 4-pentylphenyl derivative (**3c**), which has been proven to be effective against clinical VZV isolates, will be further developed as a candidate drug.[9a,c] Taking into account an interest in *p*-alkylphenyl furanopyrimidine nucleosides due to their extraordinary antiviral activity, we report the NMR conformational analysis

*Keywords*: Nucleosides; Furanopyrimidine; Conformation.
* Corresponding authors. Tel.: +1 248 3702248; fax: +1 248 3702321; e-mail: dembinsk@oakland.edu

0968-0896/$ - see front matter © 2004 Elsevier Ltd. All rights reserved.
doi:10.1016/j.bmc.2004.11.013

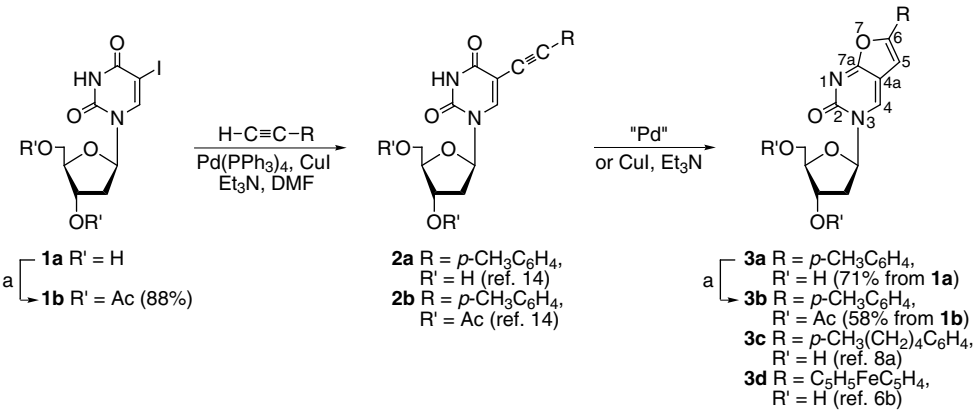


**Scheme 1.** Synthesis of furanopyrimidine nucleosides **3a** and **3b**. Reagents: (a) $Ac_2O$, pyridine.

in solution for the *p*-tolyl-substituted furanopyrimidine (**3a**). In addition, acylation of the ribose facilitated quality crystal growth, which allowed us to obtain a crystal structure for the acetyl-protected derivative **3b**.

## 2. Results and discussion

### 2.1. Synthesis

The bicyclic furopyrimidine **3** arises at elevated temperatures in the presence of Sonogashira coupling reagents,[11] via 5-*endo*-*dig* cyclization involving the C4 pyrimidine oxygen and the acetylenic bond. Although the presence of CuI/$Et_3N$ has been pointed out to be sufficient for this reaction to occur,[4c,d] relevant heteroannulation studies indicate an important role of palladium as a catalyst in this process.[12] Thus, the bicyclic nucleoside, 3′,5′-di-*O*-acetyl-3-(2′-deoxy-β-D-ribofuranosyl)-6-(4-methylphenyl)-2,3-dihydrofuro[2,3-*d*]pyrimidin-2-one (**3b**) was prepared without isolation of the alkynyl derivative (**2b**) by a one-pot Sonogashira coupling[4c,11] and cyclization reaction. 3′,5′-Di-*O*-acetyl-5-iodo-2′-deoxyuridine (**1b**)[13,14] (1.0 equiv) was combined with 4-ethynyltoluene (1.5 equiv) in the presence of $Pd(PPh_3)_4$ (0.1 equiv), CuI (0.5 equiv), and $Et_3N$ (1.8 equiv) in DMF (5 h, 80 °C, Scheme 1). Workup gave **3b** as a white powder in 58% non-optimized yield. Synthesis of nucleoside **3a** was carried out in a similar manner as reported previously,[8a] but a higher yield was achieved in our case (71% vs 17%). $^{13}C$ NMR signals for both acetylated compounds **1b** and **3b** were assigned by an examination of coupling constants between adjacent H and C atoms.

The conformational analyses for the nucleosides were carried out based on parameters defined by Altona and Sundaralingam[15] and summarized by Saenger.[16] Three parameters describe the primary features of the conformation of a pyrimidine nucleoside: the glycosidic bond torsion angle $\chi$ (C2–N1–C1′–O4′ for pyrimidine, or C2–N3–C1′–O4′ for furanopyrimidine)[17] describes the orientation of the base relative to the furanose ring; the C4′–C5′ torsion angle $\gamma$ determines the orientation of the 5′-hydroxyl group relative to the furanose ring (angle C3′–C4′–C5′–O5′); and the furanose ring puckering is specified by the pseudorotational phase angle *P*. Two major furanose ring conformations are strongly preferred for the nucleosides: C3′-*endo* and C2′-*endo*.[16]

### 2.2. NMR studies

The nuclear Overhauser effect (NOE) is useful for the assignment of closely related proton pairs, and allows for determination of preferred conformations in solution.[18] For a sample of **3a** in DMSO-$d_6$[19] 1D NOE $^1H$ NMR spectra were recorded at 20 °C. Assignments of H2″ (2.44 ppm) and H2′ (2.09 ppm) were based on NOEs to the anomeric proton, H1′. Irradiation of H1′ (6.18 ppm) resulted in a 3.83% enhancement of H2″, whereas the peak corresponding to H2′ was not significantly enhanced (<0.25%, Table 1). Strong NOEs between H6/H8 of pyrimidine/purine to H2′ and H3′ of the 2′-deoxyribose indicate that an *anti* conformation is dominant, based on the studies by Seela and co-workers.[20] In contrast, stronger NOEs exist between H6/H8 of pyrimidine/purine and H1′ when a population of *syn* conformations predominates.[20] In our experiment (results summarized in Table 1), irradiation of H4 resulted in NOEs at H1′ (0.71%), H2′ (1.20%), and H3′ (0.85%). This observation is in agreement with a reverse experiment, in which irradiation of H2′ and H3′ leads to strong NOEs at H4[17] of furanopyrimidine (7.60% and 1.48%, respectively). This data suggests that the majority of the population exists as the *anti* conformer. In addition, results of the reverse experiment of H1′ irradi-

**Table 1.** 1D NOE results for compound **3a** at 20 °C (NOEs are given in order of decreasing magnitude)

| Proton irradiated | NOE (%) |
|---|---|
| H4 | H2′ (1.20), H3′ (0.85), H5′/H5″ (0.72), H1′ (0.71) |
| H1′ | H2″ (3.83), H4′ (0.73), H4 (0.54), H2′ (0.24) |
| H2′ | H2″ (34.5), H3′ (11.35), H4 (7.60), H1′ (2.33) |
| H2″ | H2′ (31.92), H1′ (18.23), H3′ (2.89), H4′ (1.60) |
| H3′ | H2′ (4.23), H5′/H5″ (3.21), H4′ (3.04), H2″ (1.75), H4 (1.48) |

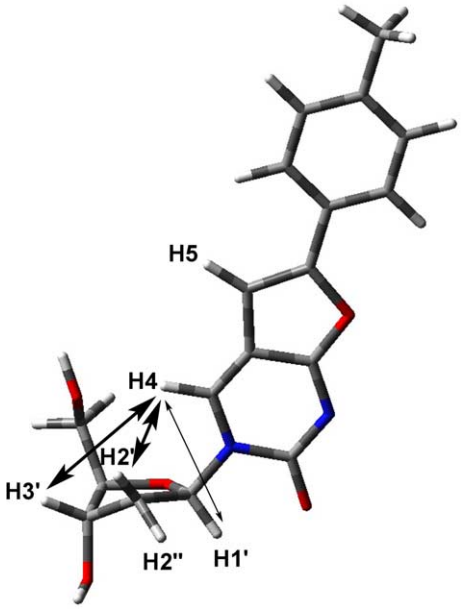


**Figure 1.** A structure representing the proposed conformation of compound **3a** as depicted by 1D NOE interactions. Thicker/thinner arrows represent stronger/weaker NOEs.

ation are in support of an *anti*-biased population because a weak NOE enhancement at H4 of 0.54% is observed. A stronger NOE at H1′ would have been indicative of the *syn* conformation. The most significant NOE interactions and the proposed conformation of compound **3a** are illustrated in Figure 1.

The sugar puckers of a nucleoside most frequently adopt either a C2′-*endo* (*S*, or south) or C3′-*endo* (*N*, or north) conformation. The dominant sugar pucker can be identified based on $J_{H1'-H2'}$ and $J_{H3'-H4'}$ coupling constants.[21] The percentages of C3′-*endo* versus C2′-*endo* are calculated from the following equations: % C2′-*endo* = $100 \times J_{1',2'}/(J_{1',2'} + J_{3',4'})$, and % C3′-*endo* = 100 − % C2′-*endo*.[21] The coupling constants observed for compound **3a** and its preferred sugar conformation are illustrated in Tables 2 and 3. The preferred C2′-*endo* conformation measured at 20 and 37 °C implies that this compound does not undergo a significant temperature-dependent conformational change.

**Table 2.** 2′-Deoxyribose $^1H$–$^1H$ coupling constants for **3a** at 20 °C

| Temp (°C) | Coupling constants $J_{H,H}$ (Hz) | | | | | | |
|---|---|---|---|---|---|---|---|
| | $J_{1',2'}$ | $J_{1',2''}$ | $J_{2',3'}$ | $J_{2'',3'}$ | $J_{3',4'}$ | $J_{4',5'}$ | $J_{4',5''}$ |
| 20 | 6.0 | 6.2 | 6.0 | 4.2 | 3.8 | 3.8 | 3.8 |
| 37 | 6.3 | 6.1 | 6.3 | 4.1 | 3.7 | 3.7 | 3.7 |

**Table 3.** Percentage of C3′-*endo* (*N*) versus C2′-*endo* (*S*) conformer and equilibrium constants (*N*/*S*) for nucleoside **3a** at 20 and 37 °C

| Temp (°C) | % C3′-*endo* (*N*) | % C2′-*endo* (*S*) | $K_{eq}$ (*N*/*S*) |
|---|---|---|---|
| 20 | 39 | 61 | 0.6 |
| 37 | 37 | 63 | 0.6 |

## 2.3. Crystallographic studies

Cyclic nucleoside **3b** was crystallized from $CHCl_3$/$CH_3OH$ (layering) as colorless needles. The detailed structure of **3b** was established by X-ray crystallography, as described in Table 4. Figure 2 shows the ORTEP views of the molecule with the numbering scheme used for analysis.[17] Two crystallographically independent molecules (A and B) have been found in the crystallographic asymmetric unit. Structures A and B are almost identical in their geometry as evidenced by interatomic distances and bond angles and by visualization of superimposed molecules. Selected bond lengths and angles are summarized in Table 5, whereas all bond lengths, angles, equivalent and anisotropic thermal parameters, and hydrogen atom coordinates are given in the supporting information.

A search of the CCDC database revealed few crystallographically characterized compounds with atom connectivity relevant to the bicyclo furanopyrimidine motif. Most of them embody a hydrogenated double bond of the furan unit, thus are not congruent. When multiplicity of the bond system is strictly taken into account, only two recently reported structures remain pertinent. Structural features of the furanopyrimidine base (**4**),[6a] and the entire nucleoside (**3d**),[6b] both ferrocene-substituted at C6, were compared with our data for **3b**.

**Table 4.** Summary of crystallographic data for **3b**

| | |
|---|---|
| Molecular formula | $C_{22}H_{22}N_2O_7$ |
| Molecular weight | 426.42 |
| Crystal system | Monoclinic |
| Space group | $P2_1$ |
| Temperature of collection (K) | 100(1) |
| Cell dimensions [100(1) K] | |
| $a$, Å | 6.666(1) |
| $b$, Å | 12.225(1) |
| $c$, Å | 24.676(2) |
| $\alpha$, deg | 90.00(1) |
| $\beta$, deg | 90.24(1) |
| $\gamma$, deg | 90.00(1) |
| $V$, Å$^3$ | 2010.9(4) |
| $Z$ | 4 |
| $d_{calc}$, g/cm$^3$ (100(1) K) | 1.409 |
| Crystal dimensions, mm | $0.4 \times 0.2 \times 0.2$ |
| Diffractometer | KUMA KM4 CCD |
| Radiation $\lambda$ | MoK$\alpha$ (0.71073 Å) |
| Data collection method | $\omega$ scan |
| Reflections measured | 12,736 |
| Range/indices ($h$, $k$, $l$) | −8, 7; −15, 16; −32, 31 |
| $\theta$ limit, deg | 3.43–28.44 |
| Total no. of unique data | 8384 |
| No. of observed data, $I > 2\sigma$ ($I$) | 5854 |
| No. of variables | 566 |
| No. of restraints | 1 |
| $R_{int}$ | 0.0267 |
| $R = \Sigma\|\|F_o\|-\|F_c\|\|/\Sigma\|F_o\|$ (all, observed) | 0.0720, 0.0437 |
| $wR_2 = (\Sigma[w(F_o^2 - F_c^2)^2]/\Sigma w[F_o^4])^{1/2}$ (all, observed) | 0.0791, 0.0709 |
| $\Delta/\sigma$ (max) | 0.275 |
| $\Delta\rho$ (max), e/Å$^3$ | 0.217 |

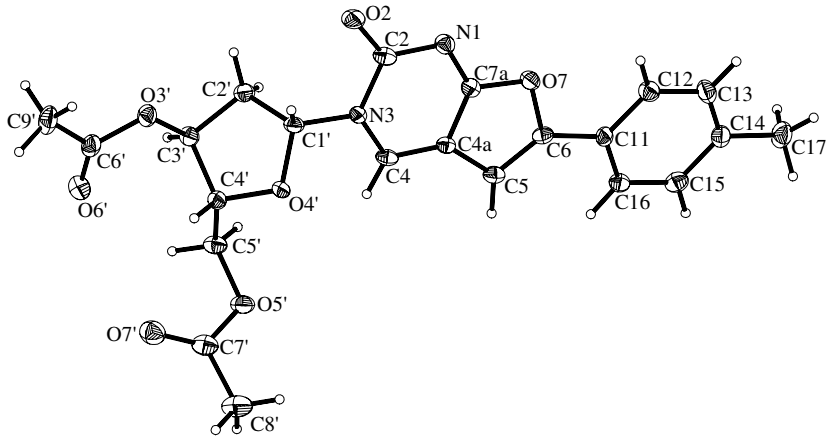


**Figure 2.** A view of the molecular structure of **3b** with the crystallographical atom-labeling scheme. Displacement ellipsoids are drawn at 50% probability level.

**Table 5.** Selected bond lengths (Å) and bond angles (deg) for molecules A and B of **3b**, numbering used as for molecule A

| | | | | | |
|---|---|---|---|---|---|
| O2–C2 | 1.236(3) | 1.237(3) | N3–C1′ | 1.483(3) | 1.484(3) |
| O7–C6 | 1.431(3) | 1.427(3) | C4–C4a | 1.359(4) | 1.353(4) |
| O7–C7a | 1.360(3) | 1.360(3) | C4a–C5 | 1.448(3) | 1.439(5) |
| O3′–C3′ | 1.461(3) | 1.457(3) | C4a–C7a | 1.441(3) | 1.412(3) |
| O4′–C1′ | 1.420(2) | 1.428(3) | C5–C6 | 1.346(3) | 1.352(3) |
| O4′–C4′ | 1.444(3) | 1.445(3) | C6–C11 | 1.459(3) | 1.451(4) |
| O5′–C5′ | 1.445(3) | 1.451(3) | C1′–C2′ | 1.517(3) | 1.519(3) |
| N1–C2 | 1.375(3) | 1.380(3) | C2′–C3′ | 1.508(3) | 1.508(3) |
| N1–C7a | 1.310(3) | 1.309(3) | C3′–C4′ | 1.529(3) | 1.533(3) |
| N3–C2 | 1.428(3) | 1.426(3) | C4′–C5′ | 1.514(3) | 1.510(3) |
| N3–C4 | 1.363(3) | 1.364(3) | | | |
| O2–C2–N1 | 123.5(2) | 122.7(2) | C2–N1–C7a | 115.6(2) | 114.8(2) |
| O2–C2–N3 | 118.7(3) | 118.9(2) | C2–N3–C4 | 123.7(2) | 123.4(2) |
| O7–C6–C5 | 111.5(2) | 111.2(2) | C2–N3–C1′ | 114.39(19) | 114.5(2) |
| O7–C6–C11 | 114.6(2) | 114.8(2) | C4–N3–C1′ | 121.9(2) | 122.0(2) |
| O7–C7a–N1 | 120.4(2) | 119.9(2) | C4–C4a–C5 | 138.3(2) | 138.4(2) |
| O7–C7a–C4a | 110.4(2) | 110.4(2) | C4–C4a–C7a | 115.3(2) | 115.3(2) |
| O3′–C3′–C2′ | 108.78(18) | 108.57(18) | C5–C4a–C7a | 106.4(2) | 106.3(2) |
| O3′–C3′–C4′ | 110.9(2) | 111.0(2) | C5–C6–C11 | 134.0(2) | 134.0(2) |
| O4′–C1′–N3 | 107.89(18) | 107.94(18) | C6–O7–C7a | 105.52(18) | 105.59(18) |
| O4′–C1′–C2′ | 106.60(18) | 106.50(19) | C6–C5–C4a | 106.3(2) | 106.5(2) |
| O4′–C4′–C3′ | 107.10(19) | 106.83(18) | C6–C11–C12 | 121.2(2) | 120.9(2) |
| O4–C4′–C5′ | 109.55(19) | 109.49(19) | C6–C11–C16 | 120.4(2) | 120.5(2) |
| N1–C2–N3 | 117.8(2) | 118.3(2) | C1′–O4′–C4′ | 110.24(17) | 110.36(17) |
| N1–C7a–C4a | 129.2(3) | 129.6(3) | C1′–C2′–C3′ | 104.5(2) | 104.42(19) |
| N3–C4–C4a | 118.3(2) | 118.4(2) | C2′–C3′–C4′ | 104.7(2) | 105.1(2) |
| N3–C1′–C2′ | 113.1(2) | 113.2(2) | C3′–C4′–C5′ | 113.0(2) | 113.4(2) |

The 2′-deoxyribose ring in **3b** crystallizes in the C2′-*endo* conformation, dominant for the 2′-deoxyribose series, with the pseudorotational phase angle $P = 150.4/150.8°$ (for molecules A and B, average 150.6°),[22] thus locating the conformation as $^{2}T_{1}$ between twist $^{2}_{1}T$ and envelope $^{2}E$. By comparison, the furanose rings in **3d**, adopt a relatively close conformation with $P = 186.0/193.5°$ (average 189.8°, $_{3}T^{2}$ conformation) for (O1′/O1′A)[23] rings; a very minor contribution of C3′-*exo* can be noticed. The ring-puckering Cremer and Pople[24] parameters are $q = 0.252(2)$ and $\varphi = 63.3(3)°$ and $q = 0.251(2)$ and $\varphi = 62.8(5)°$ for the rings of A/B molecules of **3b**. The same parameters calculated for two crystallographically independent molecules of **3d** are $q = 0.363(2)$ and $\varphi = 76.1(3)°$ and $q = 0.361(2)$ and $\varphi = 94.4(3)°$ for (O1′/O1′A)[23] rings, respectively.

The ribose–base distance, C1′–N3, is the same for crystallographically characterized furanopyrimidine nucleosides (1.483(3)/1.484(3) Å of both molecules for **3b** and 1.478(3)/1.479(2) Å for **3d**). Similar to **3a** in solution and **3d** in the crystalline state, the C2 carbonyl group of **3b** adopted an *anti* orientation toward the ribose ring: the glycosidic bond torsion angle $\chi$ (O4′-C1′–N3–C2) is −161.8(2)/−162.2(2)° (−148.0/−155.4° for **3d**). The furanopyrimidine is planar in both independent molecules of **3b**. The atoms most distorted from planarity are N3 (0.026/0.024 Å). For comparison, the most displaced

atom in **4** is C2(C23)[23] 0.030 Å. Structure **3d** combines these features—the most displaced atoms are C2 (0.043 Å) and, in the second molecule, N3(N1a)[23] (0.043 Å). The *p*-tolyl group is bound directly to the furanopyrimidine through a C6–C11 linkage 1.459(3)/1.451(4) Å with a slightly larger distance than the cyclopentadienyl ring of the ferrocene substituent in **3d/4**. The length of the newly formed double bond (C5–C6) is in a typical C=C bond range (1.346(3)/1.352(3) Å), similar to the ferrocene nucleoside **3d**, but shorter than for **4** (1.340(3)/1.340(3) and 1.379(8) Å, respectively). The base carbon–oxygen bond lengths (C2–O2 and C7a–O7, 1.236(3)/1.237(3) and 1.360(3)/1.360(3) Å) indicate similar double- and single-bond character as observed in **3d** and **4** (1.227(3)/1.231(3) and 1.224(7), and 1.350(2)/1.355(2) and 1.355(7) Å). The *p*-tolyl aromatic ring lies almost in the same plane as the bicyclic base; the dihedral angle C5–C6–C11–C16 is 8.9(4)/7.8(4)°. When considering the whole plane, the *p*-tolyl ring is twisted by 10.1/10.0° from the plane of the furanopyrimidine. When viewing the structure from the *p*-tolyl group toward the sugar, two subsequent slight twists between planes of the *p*-tolyl, the bicyclic base, and the C1′–O4′ bond are directed *R* (plus). The plane of the attached cyclopentadienyl each twist in opposite directions, for the two independent molecules of **3d**, by 10.3/14.3° (in **4** by 7.6°). This small difference is likely attributed to packing forces. The C5′–O5′ bond is *ap* to the C4′–C3′ bond, which can be visualized by the O5′–C5′–C4′–C3′ torsion angle $\gamma = 179.4(2)/179.3(2)°$ (A/B). By comparison, the free hydroxyl group of **3d** adopts a different conformation in which the $\gamma$ angle differs by ca. 115° for the two crystallographically independent molecules (69.8/60.9°).[6b] Packing diagrams and discussion are given in the Supplementary data.

The electronic absorption spectrum for **3a** was compared to the uncyclized alkynyl uridine **2a** (Fig. 3). As expected, the absorption maxima shift to longer wavelengths for the fused cyclic systems, as compared to the parent alkynyl uridine. The molar absorptivity for **3a** reaches 22,000 $M^{-1}cm^{-1}$ (281 nm). Furanopyrimidines **3a/b** exhibited a strong purple luminescence on TLC plates in UV light (254 nm); a more detailed characterization was also undertaken because fluorescent nucleosides have practical applications. An emission spectrum for **3a** is shown in Figure 3. The wavelength of the observed emission peak (430 nm, **3a**) did not vary with excitation wavelength ($\lambda_{ex}$ 290 and 375 nm), and was slightly shifted to the red by comparison to the alkynyl precursor **2a** (401 nm, data not shown).[14]

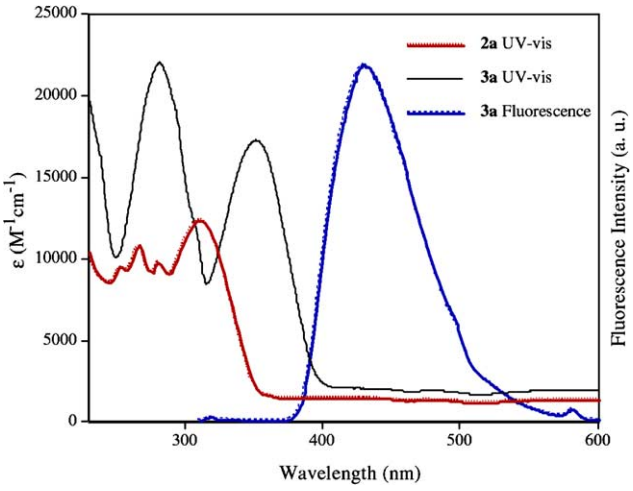


**Figure 3.** UV–vis and fluorescence ($\lambda_{ex}$ 290 nm) spectra of **3a** and comparison to the UV–vis spectrum of **2a** ($CH_3OH$).

## 3. Conclusions

In summary, we have established the conformations of an antiviral-active furanopyrimidine nucleoside by NOE NMR spectroscopy and X-ray crystallography. The solid state structure of the *p*-tolyl-substituted furanopyrimidine nucleoside **3b** is similar to the dominant solution conformation of nonacylated **3a**, and resembles the ferrocene furanopyrimidine nucleoside **3d**. The base in both **3b** and **3d** is in the *anti* position, and the deoxyribose ring is in the C2′-*endo* conformation (a minor C3′-*exo* conformation for **3d**). The aromatic rings of the *p*-tolyl and ferrocene substituents (**3b** and **3d**) lie almost in the same plane as the bicyclic base.

## 4. Experimental section

### 4.1. General

Commercial chemicals were treated as follows: DMF, distilled from $CaH_2$ and degassed (freeze and thaw) three times prior to use; $Et_3N$, distilled from $P_2O_5$; THF, distilled from Na/benzophenone; $(CH_3CO)_2O$, distilled prior to use. 5-Iodo-2′-deoxyuridine (Berry & Associates), 4-ethynyltoluene (GFS, Lancaster), tetrakis(triphenylphosphine)palladium(0) and CuI 99.999% (Aldrich), silica gel (J.T. Baker, 60–200 mesh), TLC plates (Analtech GF, cat. number 2521 or Merck 60, cat. number 5715), used as received. Other materials not listed were used as received. Progress of the reactions was monitored by TLC.

UV–visible spectra were recorded on a Cary 50 spectrometer. Fluorescence measurements were carried out on an Amico-Bowman Series 2 Luminescence Spectrometer, cells 1 and 3 mL, bandwidths of 4 nm each, PMT 650 V (24 °C). NMR spectra were obtained on Varian Unity 500, Mercury 400, or Bruker Avance 200 spectrometers. The $^1H$ and $^{13}C$ NMR chemical shifts are in $\delta$ and ppm, respectively, and $J$ values are in Hz.

### 4.2. 3-(2′-Deoxy-β-D-ribofuranosyl)-6-(4-methylphenyl)-2,3-dihydrofuro[2,3-*d*]pyrimidin-2-one (3a)[8a]

A Schlenk flask was charged with 5-iodo-2′-deoxyuridine **1a** (1.002 g, 2.830 mmol), $Pd(PPh_3)_4$ (0.654 g, 0.566 mmol), DMF (10 mL), $Et_3N$ (0.80 mL, 5.7 mmol), 4-ethynyltoluene (0.82 mL, 6.5 mmol), and CuI (0.054 g, 0.28 mmol). The mixture was stirred for 5 h at 80 °C. TLC showed complete conversion of the substrate. The solid was filtered off, the solvent removed

from the filtrate (by oil pump vacuum), and the residue kept under an oil pump vacuum for 2 h. The solid was dissolved in $CHCl_3$ (10 mL) and kept at −15 °C (freezer) for 24 h. The solid was filtered off, washed with $CHCl_3$ three times, and dried by oil pump vacuum to give **3a** as a white powder (0.687 g, 2.01 mmol, 71%). UV–vis ($CH_3OH$, $4.1 \times 10^{-5}$ M; nm, $\varepsilon$ ($M^{-1}cm^{-1}$)) 351 (17,000), 282 (22,000). Fluorescence ($CH_3OH$, $6 \times 10^{-6}$ M; nm) $\lambda_{ex}$ 290/375, $\lambda_{em}$ 430/430. NMR data matched those reported earlier.[8a]

### 4.3. 3′,5′-Di-*O*-acetyl-5-iodo-2′-deoxyuridine (1b)[13,14]

A round bottom flask was charged with 5-iodo-2′-deoxyuridine **1a** (1.000 g, 2.824 mmol), pyridine (15 mL), and $(CH_3CO)_2O$ (3.0 mL, 32 mmol). The reaction was stirred for 16 h. The solvent was removed by rotary evaporation. The residue was co-evaporated with benzene/$CH_2Cl_2$ (10/10 mL), and $CH_2Cl_2$ ($2 \times 10$ mL). The residue was dissolved in $CH_2Cl_2$ (250 mL), and washed with $NaHCO_3$ (0.5 M, $4 \times 50$ mL). The organic phase was dried over $Na_2SO_4$ and filtered. Solvent was removed by rotary evaporation. Ethanol (ca. 1.5 mL) was added and the mixture (precipitate) was kept at −20 °C (freezer) for 24 h. A white powder was collected by filtration and dried on an oil vacuum pump to give **1b** (1.085 g, 2.476 mmol, 88%).

NMR ($CDCl_3$): $^1$H (200 MHz) 8.92 (br s, 1H, N3), 7.98 (s, 1H, H6), 6.30 (dd, $J$ = 8.2, 5.7, 1H, H1′), 5.26 (dt, $J$ = 6.5, 2.1, 1H, H3′), 4.40 and 4.37 (2d, $J$ = 3.0 and 2.8, 2H, H5′), 4.33–4.28 (m, 1H, H4′), 2.56 (ddd, $J$ = 14.3, 5.7, 2.0 1H, H2′), 2.25–2.10 (m, 1H, H2′), 2.22 and 2.13 (2s, $2 \times 3$H, 2 $COCH_3$); $^{13}$C (50 MHz) 170.4 and 170.3 (2 $COCH_3$), 160.0 (d, $J$ = 9.6, C4), 150.1 (d, $J$ = 7.7, C2), 143.9 (dd, $J$ = 184.9, 3.0, C6), 85.7 (dm, $J$ = 171.6, C1′),[25] 82.5 (dm, $J$ = 151.7, C4′),[25] 74.2 (dm, $J$ = 158.3, C3′), 69.2 (d, $J$ = 4.9, C5), 64.0 (t, $J$ = 149.1, C5′), 38.5 (dd, $J$ = 138.5, 132.2, C2′), 21.3 (q, $J$ = 129.9, $COCH_3$), 21.1 (q, $J$ = 130.1, $COCH_3$).

### 4.4. 3′,5′-Di-*O*-acetyl-3-(2′-deoxy-β-D-ribofuranosyl)-6-(4-methylphenyl)-2,3-dihydrofuro[2,3-*d*]pyrimidin-2-one (3b)[26]

A Schlenk flask was charged with 3′,5′-di-*O*-acetyl-5-iodo-2′-deoxyuridine **1b** (0.389 g, 0.888 mmol), 4-ethynyltoluene (0.17 mL, 1.3 mmol), triethylamine (0.22 mL, 1.6 mmol), DMF (10 mL), $Pd(PPh_3)_4$ (0.102 g, 0.0883 mmol), and CuI (0.079 g, 0.41 mmol). The mixture was stirred at 80 °C for 3 h. DMF was removed by oil pump vacuum (water bath) and the residue was co-evaporated with $CH_3OH$ (10 mL). The residue was dissolved in $CHCl_3/CH_3OH$ (80:20) and filtered over a silica gel column ($15 \times 2$ cm). The solvent was removed by rotary evaporation. Silica gel column chromatography (hexane/EtOAc gradient, 80:20 → 65:35 → 50:50, $35 \times 2$ cm) gave a white powder that was dried under oil pump vacuum. Recrystallization from $CHCl_3/CH_3OH$ (layering) gave **3b** (0.221 g, 0.518 mmol, 58%). MS[27] ($ES^+$, KOAc, MeOH, calcd for $C_{22}H_{22}N_2O_7$ 426.1) 891 [(2M+K)$^+$, 100%], 875 [(2M+Na)$^+$, 35%], 853 [(2M+H)$^+$, 11%], 500 (unassigned, 30%), 465 [(M+K)$^+$, 90%], 449 [(M+Na)$^+$, 33%], 427 [(M+H)$^+$, 10%]; no other peaks above 250 of >5%.

NMR ($CDCl_3$): $^1$H (500 MHz) 8.27 (s, 1H, H4), 7.66 (d, $J$ = 8.0, 1H, *m*-$C_6H_4CH_3$),[28] 7.23 (d, $J$ = 8.0, 2H, *o*-$C_6H_4CH_3$),[28] 6.67 (s, 1H, H5), 6.34 (dd, $J$ = 6.0, 1.5, 1H, H1′), 5.24 (q, $J$ = 2.0, 1H, H3′), 4.45–4.40 (m, 3H, H4′, H5′), 2.98 (ddd, $J$ = 14.3, 5.5, 2.8, 1H, H2′), 2.40 (s, 3H, $C_6H_4CH_3$), 2.12 (s, 3H, $COCH_3$), 2.13–2.09 (m, 1H, H2′), 2.08 (s, 3H, $COCH_3$). $^{13}$C (ppm, 50 MHz) 172.0 (C7a), 170.7 and 170.5 (2 $COCH_3$), 156.6 (br s C6), 154.7 (C2), 140.4 (*i*-$C_6H_4CH_3$), 134.4 (d, $J$ = 184.9, C4), 129.9 (d, $J$ = 158.2, *m*-$C_6H_4CH_3$), 125.7 (*p*-$C_6H_4CH_3$), 125.2 (br d, $J$ = 156.4, *o*-$C_6H_4CH_3$), 108.7 (C4a), 96.8 (d, $J$ = 180.2, C5), 88.8 (d, $J$ = 175.3, C1′),[25] 83.5 (d, $J$ = 152.1, C4′),[25] 74.3 (d, $J$ = 158.2, C3′), 63.9 (t, $J$ = 148.7, C5′), 39.5 (dd, $J$ = 139.7, 132.8, C2′), 21.7 (q, $J$ = 126.8, $C_6H_4CH_3$), 21.1 (q, $J$ = 130.0, 2 $COCH_3$).

### 4.5. NOE studies

NMR data were acquired on a Varian Unity 500 MHz spectrometer. The sealed sample was prepared in a drybox in anhydrous DMSO-$d_6$. Each proton listed in Table 1 was irradiated for 1D NOE difference spectroscopy and resonances were acquired.

### 4.6. Crystallography

Colorless needles of **3b** were grown by solvent diffusion (layering) of a $CHCl_3$ solution with MeOH (12 days). Data were collected as outlined in Table 4 using a KUMA KM4 CCD diffractometer equipped with an Oxford Cryosystem–Cryostream cooler. Cell parameters (100(1) K) were obtained from 3820 reflections with $3.43° < \theta < 28.44°$. The space group was determined from systematic absences and subsequent least-squares refinement. One frame checked every 50 frames showed no crystal decay. Lorentz and polarization corrections were applied. The structure was solved by direct techniques with SHELXS and refined by full-matrix-least-squares on $F^2$ using SHELXL-97.[29] Nonhydrogen atoms were refined with anisotropic thermal parameters. Hydrogen atom positions were calculated and added to the structure factor calculations, but were not refined. Scattering factors, and $\Delta f'$ and $\Delta f''$ values, were taken from the literature.[30] Flack parameter for **3b** was 0.5(7).[31]

Data for **3b** (excluding structure factors) have been deposited with the Cambridge Crystallographic Data Centre as supplementary publication CCDC-249882. Copies of this information can be obtained free upon application to CCDC, 12 Union Road, Cambridge CB2 1EZ, UK. Fax: (internat.) + 44-1223/336-033; E-mail deposit@ccdc.cam.ac.uk.

### Acknowledgements

We thank the Oakland University, Research Excellence Program in Biotechnology, NIH (grants CA111329 and

GM054632), and Polish State Committee for Scientific Research (grant 4 T09A14824) for support of this research. NATO (grant PST.CLG.977371) is acknowledged for a travel award. We are also grateful to Dr. B. Ksebati for NMR assistance, S. Grossman and Prof. E. Sochacka for helpful discussions.

## Supplementary data

Supplementary data associated with this article can be found, in the online version, at doi:10.1016/j.bmc.2004.11.013. Information available: NMR spectra for compounds **3a**,**b**, interatomic distances, bond angles, coordinates and thermal parameters, packing discussion and diagram for compound **3b**; crystallographic data are also available as cif file.

## References and notes

1. See for example: (a) Grotenbreg, G. M.; Timmer, M. S. M.; Llamas-Saiz, A. L.; Verdoes, M.; van der Marel, G. A.; van Raaij, M. J.; Overkleeft, H. S.; Overhand, M. *J. Am. Chem. Soc.* **2004**, *126*, 3444–3446; (b) van Well, R. M.; Marinelli, L.; Altona, C.; Erkelens, K.; Siegal, G.; van Raaij, M.; Llamas-Saiz, A. L.; Kessler, H.; Novellino, E.; Lavecchia, A.; van Boom, J. H.; Overhand, M. *J. Am. Chem. Soc.* **2003**, *125*, 10822–10829.
2. Recent work: Marquez, V. E.; Ben-Kasus, T.; Barchi, J. J., Jr.; Green, K. M.; Nicklaus, M. C.; Agbaria, R. *J. Am. Chem. Soc.* **2004**, *126*, 543–549.
3. See for example: (a) Shealy, Y. F.; O'Dell, C. A.; Arnett, G.; Shannon, W. M. *J. Med. Chem.* **1986**, *29*, 79–84; (b) Sharma, R. A.; Kavai, I.; Hughes, R. G., Jr.; Bobek, M. *J. Med. Chem.* **1984**, *27*, 410–412; (c) De Clercq, E.; Descamps, J.; Balzarini, J.; Giziewicz, J.; Barr, P. J.; Robins, M. J. *J. Med. Chem.* **1983**, *26*, 661–666; (d) Flanagan, M. W.; Wagner, R. W. The Development of C-5 Propyne Oligonucleotides as Inhibitors of Gene Function. In *Applied Antisense Oligonucleotide Technology*; Stein, C. A., Krieg, A. M., Eds.; Wiley-Liss: New York, 1998, pp 174–191; (e) Kundu, N. G.; Mahanty, J. S.; Chowdhury, C.; Dasgupta, S. K.; Das, B.; Spears, C. P.; Balzarini, J.; De Clercq, E. *Eur. J. Med. Chem.* **1999**, *34*, 389–398.
4. (a) Robins, M. J.; Vinayak, R. S.; Wood, S. G. *Tetrahedron Lett.* **1990**, *31*, 3731–3734; (b) Cruickshank, K. A.; Stockwell, D. L. *Tetrahedron Lett.* **1988**, *29*, 5221–5224; (c) Robins, M. J.; Barr, P. J. *J. Org. Chem.* **1983**, *48*, 1854–1862; (d) Robins, M. J.; Barr, P. J. *Tetrahedron Lett.* **1981**, *22*, 421–424; (e) Crisp, G. T.; Flynn, B. L. *J. Org. Chem.* **1993**, *58*, 6614–6619.
5. Review: Korshun, V. A.; Manasova, E. V.; Berlin, Yu. A. *Bioorg. Khim.* **1997**, *23*, 324–387 (in Russian).
6. Recently reported cyclizations: (a) Coutouli-Argyropoulou, E.; Tsitabani, M.; Petrantonakis, G.; Terzis, A.; Raptopoulou, C. *Org. Biomol. Chem.* **2003**, *1*, 1382–1388; (b) Pike, A. R.; Ryder, L. C.; Horrocks, B. R.; Clegg, W.; Elsegood, M. R. J.; Connolly, B. A.; Houlton, A. *Chem. Eur. J.* **2002**, *8*, 2891–2899; (c) Yu, C. J.; Yowanto, H.; Wan, Y.; Meade, T. J.; Chong, Y.; Strong, M.; Donilon, L. H.; Kayyem, J. F.; Gozin, M.; Blackburn, G. F. *J. Am. Chem. Soc.* **2000**, *122*, 6767–6768.
7. (a) 5-(2-Bromovinyl)uracil undergoes cyclization with *t*-BuOK: Bleackley, R. C.; Jones, A. S.; Walker, R. T. *Tetrahedron* **1976**, *32*, 2795–2797; (b) $AgNO_3$ (cat.) cyclization: Aucagne, V.; Amblard, F.; Agrofoglio, L. A. *Synlett* **2004**, 2406–2408; (c) NIS/NBS halocyclization: Rao, M. S.; Esho, N.; Sergeant, C.; Dembinski, R. *J. Org. Chem.* **2003**, *68*, 6788–6790.
8. (a) McGuigan, C.; Barucki, H.; Blewett, S.; Carangio, A.; Erichsen, J. T.; Andrei, G.; Snoeck, R.; De Clercq, E.; Balzarini, J. *J. Med. Chem.* **2000**, *43*, 4993–4997; (b) Brancale, A.; McGuigan, C.; Andrei, G.; Snoeck, R.; De Clercq, E.; Balzarini, J. *Bioorg. Med. Chem. Lett.* **2000**, *10*, 1215–1217; (c) McGuigan, C.; Yarnold, C. J.; Jones, G.; Velázquez, S.; Barucki, H.; Brancale, A.; Andrei, G.; Snoeck, R.; De Clercq, E.; Balzarini, J. *J. Med. Chem.* **1999**, *42*, 4479–4484; (d) Srinivasan, S.; McGuigan, C.; Andrei, G.; Snoeck, R.; De Clercq, E.; Balzarini, J. *Nucleosides, Nucleotides, Nucleic Acids* **2001**, *20*, 763–766; (e) Bidet, O.; McGuigan, C.; Andrei, G.; Snoeck, R.; De Clercq, E.; Balzarini, J. *Nucleosides, Nucleotides, Nucleic Acids* **2003**, *22*, 817–819; (f) McGuigan, C.; Brancale, A.; Andrei, G.; Snoeck, R.; De Clercq, E.; Balzarini, J. *Bioorg. Med. Chem. Lett.* **2003**, *13*, 4511–4513; (g) McGuigan, C.; Carangio, A.; Snoeck, R.; Andrei, G.; De Clercq, E.; Balzarini, J. *Nucleosides, Nucleotides, Nucleic Acids* **2004**, *23*, 1–5; (h) McGuigan, C.; Pathirana, R. N.; Snoeck, R.; Andrei, G.; De Clercq, E.; Balzarini, J. *J. Med. Chem.* **2004**, *47*, 1847–1851.
9. Reviews: (a) De Clercq, E. D. *Med. Res. Rev.* **2003**, *23*, 253–274; (b) Balzarini, J.; McGuigan, C. *Biochim. Biophys. Acta* **2002**, *1587*, 287–295; (c) Balzarini, J.; McGuigan, C. *J. Antimicrob. Chemother.* **2002**, *50*, 5–9; (d) McGuigan, C.; Brancale, A.; Barucki, H.; Srinivasan, S.; Jones, G.; Pathirana, R.; Carangio, A.; Blewett, S.; Luoni, G.; Bidet, O.; Jukes, A.; Jarvis, C.; Andrei, G.; Snoeck, R.; De Clercq, E.; Balzarini, J. *Antiviral Chem. Chemother.* **2001**, *12*, 77–89; (e) McGuigan, C.; Brancale, A.; Barucki, H.; Srinivasan, S.; Jones, G.; Pathirana, R.; Blewett, S.; Alvarez, R.; Yarnold, C. J.; Carangio, A.; Velázquez, S.; Andrei, G.; Snoeck, R.; De Clercq, E.; Balzarini, J. *Drugs Future* **2000**, *25*, 1151–1161.
10. (a) McGuigan, C.; Velázquez, S.; De Clercq, E.; Balzarini, J. *Antiviral Chem. Chemother.* **1997**, *8*, 519–527; (b) McGuigan, C.; Camarasa, M.-J.; Egberink, H.; Hartmann, K.; Karlsson, A.; Perno, C.-F.; Balzarini, J. *Int. Antiviral News* **1997**, *5*, 19–21.
11. (a) Sonogashira, K. *J. Organomet. Chem.* **2002**, *653*, 46–49; (b) Sonogashira, K. Cross-coupling Reactions to sp Carbon Atoms. In *Metal-Catalyzed Cross-Coupling Reactions*; Sonogashira Diederich, F., Stang, P. J., Eds.; Wiley-VCH: Weinheim, 1998, pp 203–230.
12. (a) Zeni, G.; Larock, R. C. *Chem. Rev.* **2004**, *104*, 2285–2309; (b) Larock, R. C. Palladium-Catalyzed Annulation. In *Perspectives in Organopalladium Chemistry for the XXI Century*; Tsuji, J., Ed.; Elsevier: Lausanne, Switzerland, 1999; pp 111–124; (c) Larock, R. C. *Pure Appl. Chem.* **1999**, *71*, 1435–1442; (d) Larock, R. C. *J. Organomet. Chem.* **1999**, *576*, 111–124; (e) Kel'in, A. V.; Gevorgyan, V. *J. Org. Chem.* **2002**, *67*, 95–98.
13. Chang, P. K.; Welch, A. D. *J. Med. Chem.* **1963**, *6*, 428–430.
14. Esho, N.; Davies, B.; Lee, J.; Dembinski, R. *Chem. Commun.* **2002**, 332–333.
15. Altona, C.; Sundaralingam, M. *J. Am. Chem. Soc.* **1972**, *94*, 8205–8212.
16. Saenger, W. *Principles of Nucleic Acids Structure*; Springer Verlag: New York, 1984, pp 1–82; For definition of angles see: Seeman, N. C.; Rosenberg, J. M.; Suddath, F. L.; Park Kim, J. J.; Rich, A. *J. Mol. Biol.* **1976**, *104*, 142–143.
17. Numbering of the six-membered ring for furanopyrimidine used in this work differs from the parent pyrimidine (uridine) ring and follows RF 10623: *Ring Systems Handbook*, American Chemical Society, Chemical Abstracts Service: Columbus, 1993; p 498RSF.

18. See for example: Neuhaus, D.; Williamson, M. P. *The Nuclear Overhauser Effect in Structural and Conformational Analysis*; Wiley-VCH: New York, 2000; pp 1–619.
19. Hart, P. A.; Davis, J. P. *J. Am. Chem. Soc.* **1972**, *94*, 2572–2577.
20. Rosemeyer, H.; Tóth, G.; Golankiewicz, B.; Kazimierczuk, Z.; Bourgeois, W.; Kretschmer, U.; Muth, H.-P.; Seela, F. *J. Org. Chem.* **1990**, *22*, 5484–5790.
21. Altona, C.; Sundaralingam, M. *J. Am. Chem. Soc.* **1973**, *95*, 2333–2344.
22. Calculated from tan $P = [(v_4 + v_1)-(v_3 + v_0)]/2v_2$ (sin 36° + sin 72°).
23. Numbering used in original reference given in parentheses.
24. Cremer, D.; Pople, J. A. *J. Am. Chem. Soc.* **1975**, *97*, 1354–1358.
25. Chemical shifts for C-1′ and C-4′ of **1b**, **3b** were assigned based on coupling constants. We attributed larger $J_{CH}$ (171.6, 175.3 vs 151.7, 152.1 Hz) of these close signals to C-1′. A gHMQC spectrum for **3a** (Supplementary data) shows cross peaks for $^{13}C$ signals of 88.8 ppm with H-4′ and 88.3 ppm with H-1′ proton.
26. Acetylation of **3a** (20 mg), according to the procedure similar to that for **1b** in the presence of 4-dimethylaminopyridine (cat.), gave **3b** that showed satisfactory purity by $^{1}H$ and $^{13}C$ NMR.
27. *m*/*z* for most intense peak of isotope envelope.
28. The *p*/*m*/*o*/*i* positions are assigned with respect to the $CH_3$ group.
29. Sheldrick, G. M. SHELXL-97. University of Göttingen, Germany, 1997.
30. Cromer, D. T.; Waber, J. T. In *International Tables for X-ray Crystallography*; Ibers, J. A., Hamilton, W. C., Eds.; Kynoch: Birmingham, England, 1974; Vol. 4, pp 72–98, 149–150; Tables 2.2B and 2.3.1.
31. Flack, H. D. *Acta Cryst.* **1983**, *A39*, 876–881.